Temporal Feature-Based Classification Into Myocardial Infarction and Other CVDs Merging CNN and Bi-LSTM From ECG Signal

Monisha Dey, *Member, IEEE*, Nuzaer Omar, *Member, IEEE*, and Muhammad Ahsan Ullah, *Member, IEEE*

***Abstract*—Heart attack else wise termed as myocardial infarction (MI) causes irreparable death of cardiac muscles yielding the focal reason for most casualties among all cardiovascular diseases (CVDs'). A 12-lead electrocardiogram (ECG) generally depicts cardiac abnormalities and so customary deep learning (DL) approaches use the whole signal for binary detection purposes, that is separating healthy control (HC), and MI classes. This paper proposes an alternative approach where 21 temporal features in lieu of the temporal signal are collected from the 12 lead data to reduce redundancy and class imbalance keeping the vital information intact. Then these extracted features are fed into a detection model consisting of a one dimensional (1-D) convolutional neural network (CNN) and a bidirectional long short-term memory (bi-LSTM) layer which classifies into three classes, namely: HC, MI, and non-myocardial infarction (non-MI) subjects for a realistic and reliable assessment. The model's performance is evaluated using 517 records acquired from the Physikalisch-Technische Bundesanstalt (PTB) database and a state-of-art overall accuracy of 99.246%, kappa of 0.983, and macro averaged F1 score of 98.86% were achieved using stratified 5-fold cross-validation. DL methods suffer to make unbiased decisions in the case of class imbalance due to an insufficient amount of data for a particular class and thus temporal features are employed to inherently reduce this problem. The successful performance of the extracted features depends on the precise detection of fiducial points, and so multiple novel algorithms have been introduced in this paper.**

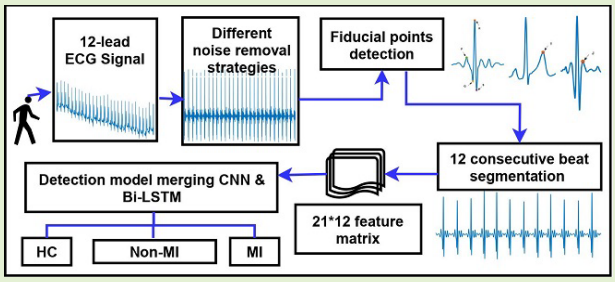

***Index Terms*—Bidirectional long short-term memory, convolutional neural network, electrocardiogram (ECG), feature extraction, myocardial infarction.**

I. Introduction

WORLD Health Organization (WHO) speculates about 24.2 million people will die from cardiovascular diseases (CVDs) by 2030, constituting 32.5% of all global deaths [1]. This is an utmost concern for the low and middle-income countries as they suffer from over 75% of the total CVD deaths. Approximately, myocardial infarction (MI) or heart attack and stroke accounts for 85% of the total CVD deaths [2]. On top of that, in both the developing and developed countries, about 40% to 75% of victims die before receiving any treatment [3]. These untimely deaths can be averted to an extent by early and explicit detection of CVDs. The experts notice the different physical and morphological changes in the electrocardiogram (ECG) that arises because of the prevalence of CVD. Irregularity in ECG is identified by a deviation of the fiducial peaks (P, Q, R, S, and T) or inconsistency in the segment intervals. Manual analysis of the signal is perplexing and calls for years of practice due to its minute value and duration. Automatic detection will not solely work as a second opinion for the professionals however conjointly extract adequate and pertinent features from it. Subsequently, automated detection and evaluation of ECG signals have gained recognition amongst researchers.

Manuscript received March 26, 2021; accepted May 7, 2021. Date of publication May 11, 2021; date of current version October 1, 2021. The associate editor coordinating the review of this article and approving it for publication was Prof. Kea-Tiong Tang. *(Monisha Dey and Nuzaer Omar contributed equally to this work.) (Corresponding author: Monisha Dey.)*

The authors are with the Department of Electrical and Electronic Engineering, Chittagong University of Engineering and Technology (CUET), Chattogram 4349, Bangladesh (e-mail: 1997monishadey@gmail.com; nnuzaeromar@gmail.com; ahsan@cuet.ac.bd).

Digital Object Identifier 10.1109/JSEN.2021.3079241

A. Literature Review

Almost all of the prevailing studies focus on a binary classification that is separating healthy subjects from MI subjects. But in reference [4], they introduced an automated multi-lead diagnostic approach where a non-MI class along with three severity levels of MI and Healthy Control (HC)

were detected using recurrent neural network (RNN) based on attention mechanism. The overall accuracy of 97.79% was accomplished using an RNN block to sequentially encode the temporal variations, an intra-lead attention block to acquire the lead-attentive illustrations, and an inter-lead attention block to integrate the vectors to obtain a high-level feature vector. A total of 14260 segments were extracted of 4-second length from the 12 leads of 372 subjects.

The other studies which utilized Physikalisch-Technische Bundesanstalt (PTB) database to classify HC and MI subjects can be broadly classified into deep learning (DL) strategies and machine learning (ML) algorithms. Most of the ML strategies extract handcrafted features employing commonly used classifiers like support vector machine (SVM) [5]–[9], K-nearest neighbors (KNN) [6], [9]–[12], artificial neural network (ANN) [11], [13], Random Forest [14] and radial basis function (RBF) [9], [13]. Some studies included classifiers like hidden Markov model (HMM) [15], threshold-based classification rule and logistic regression [16], and Levenberg–Marquardt neural network (LMNN) [6]. These handcrafted features are extracted on their statistical and morphological nature. Different studies extracted various morphological features such as ST segment [5], [7], [10], [11], T wave amplitude [7], [10], QRS complex [7], T wave and total integral [13] etc. and statistical features such as entropy [7], [8], [12], [15], skewness and kurtosis [8], [11], multiscale wavelet energy and eigen value of multiscale covariance matrices [9] were effectively captured. The existing methods for the most part utilize supervised learning algorithms whereas, reference [5] is seen to automatically detect MI without labeling any heartbeats. They applied a multiscale energy and eigenspace (MEES) method that assigns larger weights to the anomalous heartbeats compared to the regular heartbeats as it contributes heavily to the classification of MI. Nevertheless, supervised approaches have the advantage of better learning of intra-ECG differences. In reference [10], they eliminated redundant data without compromising accuracy by utilizing the pruning method.

To avoid the complexity of feature extraction and unavailability of well-established methods for detecting fiducial points, reportedly, DL approaches have gained tremendous popularity. Among the prevalent strategies, convolutional neural network (CNN) [17]–[22], and long short-term memory (LSTM) with a combination of CNN [23]–[25] have widespread use in detection of MI. Amongst the other papers, reference [26] used a combination of CNN and residual blocks, reference [27] used staked sparse autoencoders, and bidirectional gated recurrent unit [28] was used for an effective diagnosis. A wider framework as proposed by [17] was such that each of the 12 leads was represented individually as a feature branch by convolutional and pooling layer and thus had a shallower network. A real-time micro embedded system was proposed by [18] where raw heartbeats were processed using Fuzzy Information Granulation (FIG) and for detection sub 2-D CNN along with Lead Asymmetric Pooling (LAP) was employed. Another real-time based system [29] processed ECG and then consecutively transmitted, extracted feature and finally employed Rotation Forest to achieve the highest performance which reduced complexity and overall execution time than the classical approaches. Due to the presence of temporal association of ECG segments, reference [24] employed an LSTM network connected to a convolutional network for better learning of the spatial and temporal features. In [30], they utilized DL methods for learning features and employed several ML classifiers, among which SVM [30], [31] performed the best.

B. Inclusion of Non-MI Class

Prevailing studies are directed towards classifying healthy subjects from MI patients which from a practical viewpoint may result in an over or under treatment. Incorporation of a new non-MI class which includes a diagnosis of other CVDs aside from MI and healthy control (HC) can be a strategy to prevent this mistreatment [4]. Eventually, the framework designed in this paper expects to categorize the subjects into three discrete classes.

C. Importance of 12-Lead ECG

Single-lead ECG monitors are frequently used for their profoundly productive nature, reduced execution time and low expense [32]. However, single-lead ECG can not capture all the sufficient information due to the large diversity of CVD traits that might cause misdiagnosis [25]. Whereas, all 12-lead ECG data provide a better understanding of inter-lead relationships and deliver diverse information on distinctive areas of the heart yielding substantial features. Hence, this 12-lead framework has been preferred over the single-lead approach.

D. Alternate Approach by Feature Learning

Deep learning has made revolutionary advances as it possesses automatic feature learning ability from input raw data as mentioned above. It is very strenuous to extract the exclusive ECG features as with the slightest motion of the patient, unnecessary noises corrupt the signal quality. In addition to this, noises from muscle, power line interference, and baseline wandering make the ECG signal extremely noise sensitive [33]. Besides, all the input raw information may not be significant for the model to be trained. Moreover, these redundant data may cause an increase in a number of training parameters, memory usage, complexity, and processing time. If only the salient information can be retrieved and fed into the deep learning model, a lot of complications can be avoided. A lot of significant information can be recovered from ECG signals as it is an indicator of the condition of the heart, location of the anomaly, stages of severity, and evolution of heart diseases. If these information can be realized in the form of a feature matrix, it will help the experts in choosing medication and treatment. Extraction of precise time-domain features can be ensured by meticulous detection of fiducial points.

At such conditions, the outline proposed initially preprocesses the signal to remove noise by numerous filters. Then, the Pan Tompkins algorithm [34] is used for locating R peaks. Novel algorithms for detection of other fiducial

TABLE I
SELECTED RECORDS FOR EVALUATION FROM PTB DATABASE

Diagnosis	#Patients[a]	#Records
HC	52	80
non-MI	68	70
MI	148	367
Total	268	517

[a]#: number of

points which are also applied in our recent work [35] are employed and after that, 12 consecutive beats were segmented. Next, 21 time-domain features are extricated from the ECG signal after segmentation in the form of an input matrix. This input matrix is at last fed to a detection model which is comprised of CNN and bidirectional LSTM (bi-LSTM) network with stratified 5-fold cross-validation. This approach supports feature selection strategies that encompass a way better understanding of information and simplifies the system. The significant contributions of the paper are as follows:

- Classification into MI, HC and non-MI subjects ensuring greater applicability on practical purpose.
- Alternate feature learning method for minimizing redundancy from the 12-lead ECG signals.
- Application of simplified novel mathematical algorithms for locating fiducial points.

The order of the further sections is assembled as follows. Section II represents the overall working procedure for multi-class classification of subjects. In Section III, the experimental results are examined briefly. Finally, the paper is concluded with the probable future scopes of this work in section IV.

II. MATERIALS AND METHODS

This section elaborately discusses the proposed framework included in the abstract in a stepwise aspect.

A. Data Collection

For training and testing of our suggested method, 12-lead ECG data has been procured from the open-access Physikalisch-Technische Bundesanstalt (PTB) database [36], available in Physionet [37]. The 12 leads include limb leads I, II, III, aVR, aVL, and avF, and chest leads V1-V6 which corresponds to different portions of the heart. The ECG waveform with a resolution of 16 bit, has a variation in amplitude of about the range $\pm$16.384 mV. The database included 290 individuals in a total of which 22 subjects were unlabeled. Here, 517 records from the remaining 268 individuals were utilized to tell apart the 52 HC, 68 non-MI, and 148 MI subjects. The non-MI diseases include dysrhythmia, cardiomyopathy/heart failure, valvular heart disease, bundle branch block (BBB), myocarditis, and myocardial hypertrophy. The entire details of the class-wise distribution are listed in Table I.

B. Fiducial Points Detection Algorithms

The QRS complex which is visually a very prominent part of the ECG signal has to be identified initially followed by locating the other fiducial points.

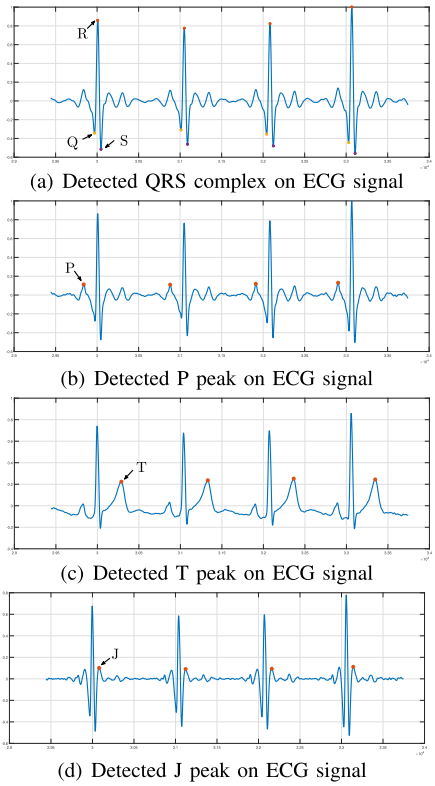

(a) Detected QRS complex on ECG signal
(b) Detected P peak on ECG signal
(c) Detected T peak on ECG signal
(d) Detected J peak on ECG signal

Fig. 1. Different fiducial points detected on ECG signal.

1) QRS Detection: The QRS complex of ECG depicts the contraction of ventricular muscles. It has a usual duration of about 0.08-0.11 s [38]. A QRS wider than usual is an indication of BBB and ventricular hypertrophy. Again, true posterior MI is recognized by the increased R wave amplitude, its duration, and high voltage QRS. The Q wave that is deeper than 2 mV and broader than 0.04 s is called a pathological Q wave if it is present in more than 1 lead. Pathological Q wave is the archetypal cause of MI and it is also seen in ventricular hypertrophy, heart failure, and left BBB.

Some of the prevailing studies use a wavelet-based technique to extract relevant QRS information. Wavelet transform finds the abrupt changes in the frequency domain at a definite point of time but proper ratios and wavelet function are the prerequisites for the timescale decomposition. Again, discrete wavelet transform (DWT) lacks proper phase information, shows poor directionality, and shift sensitivity. In accordance with these information, most strategies use Pan-Tompkins algorithm [34] to correctly detect R peak which has an accuracy of 99.325% [28]. Similarly, the proposed method in this paper also uses the Pan-Tompkins algorithm for the identification of the R peaks which is presented sequentially in Fig. 2. At last, Q and S peaks are detected using simple algorithms by applying pre and post windows to the R peak within the same frequency range. The QRS complex of a MI subject as identified by following these steps is shown in Fig. 1(a).

2) P Point Detection: The first positive deflection that occurs during atrial contraction is called P wave and is visually prominent in lead II and V1. The P wave generally has a duration that is lower than 0.12 s [39]. During inferior MI,

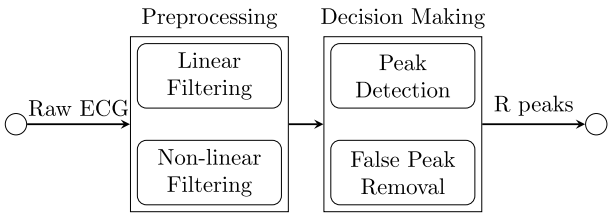

Fig. 2. Algorithm for detection of R peaks.

myocarditis, and hypertrophy, etc. the PR interval is seen to be greater than 0.2 s [38]. For the extraction of the P wave, a third-order butter-worth IIR band-pass filter in the frequency range of 5 to 30 Hz [40] is applied. A window-based approach similar to the one used for Q and S points is applied in locating peak P.

This simple approach was unable to satisfy the condition for notched P peaks and so, a further modification was done for generalization. A second peak in the same window was searched and then checked whether it lied in the amplitude difference less than 0.15 mV and time difference of $\pm$50 ms. If it satisfies both time and amplitude conditions of being a notched P peak, their location and amplitude were averaged. The detected P peak for an MI subject can be seen from Fig. 1(b).

3) T Point Detection: A T wave lies in the lower frequency range representing ventricular repolarization. It is usually less than 5 mm and 10 mm in limb and chest leads respectively. Abnormality of T wave is seen with its inversion or high amplitude in the cardiac cycle. Inversion of T waves is a vital sign of MI, cardiomyopathy, BBB, ventricular hypertrophy [38]. Tall T-waves or hyperacute T waves that peaks within half an hour can lead to ST-elevation MI [41]. Also, it is one of the key features for the diagnosis of ventricular hypertrophy and true posterior MI.

A third-order butter-worth IIR band-pass filter from 0.5 to 50 Hz and a moving average filter is used for the elimination of baseline wandering noise (0.5 to 0.6 Hz) and random noises. Initially, T peak is extracted from an ECG cycle by squaring and the similar window method used previously. The amplitude of T can be very small in some of the cases which results in a very high possibility for detection of false T peaks. Consequently, we designed a novel algorithm as presented stepwise in Fig. 3 to remove the false T peaks. After the false T removal step, finally, the actual T peak of an MI subject is evident in Fig. 1(c).

4) J Point Detection: Abnormalities in the ST segment that is its elevation or depression can indicate MI, BBB, and ventricular hypertrophy [42]. To deduce the extent of ST deviation, J point detection is mandatory. J point links the ST segment and QRS complex. J points' location after the QRS complex lacks definition and is yet inconclusive. J point is searched from 20 ms after S point in a window of 60 to 80 ms [43]. Due to its vague and uncertain nature, there are no established strategies of detection. As such, a novel derivation based approach is designed which is demonstrated in Fig. 4. J wave of an MI subject on segmented ECG after application of the algorithm is displayed in Fig 1(d).

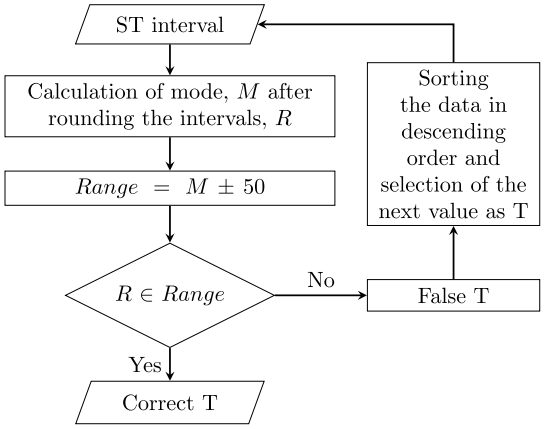

Fig. 3. Algorithm for removal of false T peaks.

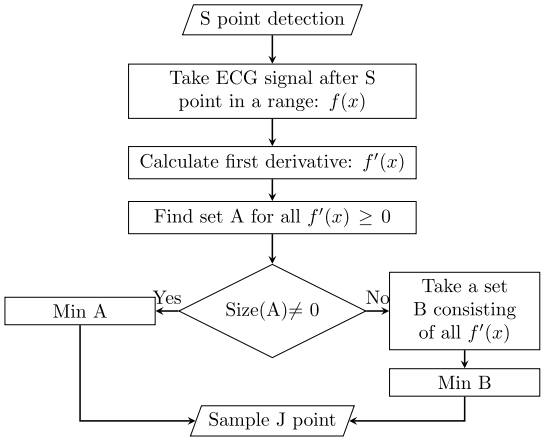

Fig. 4. Algorithm for detection of J point.

C. Feature Extraction

A 24 hours ECG recording incorporates over 100000 heartbeats [5], which not only would take an ample amount of time to process during the automated feature learning process, but also will result in massive inclusion of redundant data. These redundancies may create a computational burden in some cases. Again, most researchers used the beat segmentation method. However CVDs each MI and non-MI, are progressive in nature i.e., they require several consecutive beats for diagnosis. So, during this approach, instead of using a single beat as input, 12 sequential beats are used which considers both inter and intra-beat relations to extract the features. Initially, 32 temporally related features were extracted and after trial and error, 21 features from 12-lead ECG signal were selected for best optimization. These features were chosen from morphological and statistical outlook. These features include average intervals of QRS, PR, QT, corrected QT, ST, heart rates (maximum, minimum, mean), etc. Root mean squared deviation (RMSD) of several intervals like PR, QT, corrected QT and ST are also utilized. Amplitudes of T that may be tall or inverted in different leads are a vital indicator of CVDs derived from an MI subject as projected in Fig. 5(a) and Fig. 5(b), ST segment deviation as designated in Fig. 5(c), pathological Q wave is also included in the feature matrix [38]. Features like the number of maximas between T and Q, the average area under the curves: QRS and ST, and

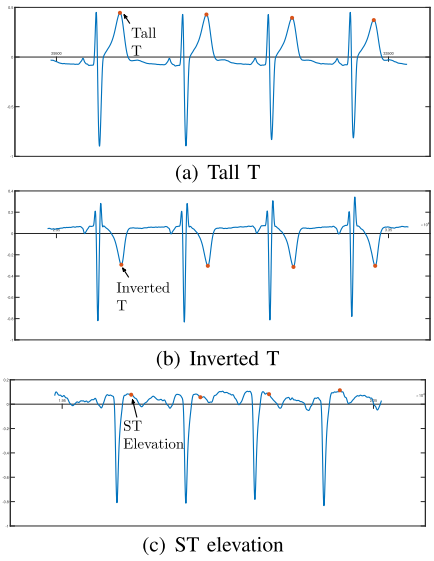

(a) Tall T

(b) Inverted T

(c) ST elevation

Fig. 5. Crucial features detected of an MI subject.

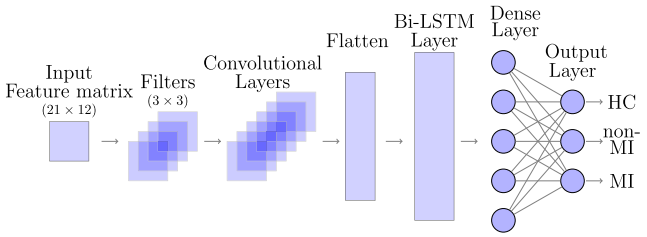

Fig. 6. A brief framework of the proposed detection model.

the ratio of both areas, age, and gender of subjects are used from [44]. Since these features contemplate the composition of ECG signals, the model can analyze other CVDs even though it is trained with an insufficient amount of data.

D. Detection Model

While most of the studies used a deeper network with around 11 to 16 computational layers [20], [22]–[24], the proposed model in this paper is very shallow with only a single 1-D CNN layer and a bi-LSTM layer. This model gets the best out of the feature matrix as the CNN layer extracts high spatial features and the bi-LSTM layer reflects the temporal relationship involved between the ECG leads. The basic framework of the model combining CNN and bi-LSTM layer is demonstrated in Fig 6. The CNN learns spatial features using the convolution method i.e., the hidden layer convolutes with the input feature matrix from the previous layer and maps the output. If x_j^l and x_i^{l-1} are the i^{th} input feature and j^{th} output feature map of the layer l, the functioning of a 1-D convolutional layer is as follows:

$$x_j^l = F(b_j^l + \sum_{i \in M_j} x_i^{l-1} * w_{ij}^l) \tag{1}$$

where M_j is the consecutive inputs to the layer, b_j^l is the associated bias and w_{ij}^l is the kernel connecting them. F represents the activation function and since rectified linear unit (ReLU) deals well with overfitting issues by converging swiftly; it is used here and the function is represented as follows:

$$F = \begin{cases} 0 & \text{for} \quad x < 0 \\ x & \text{for} \quad x \geq 0. \end{cases} \tag{2}$$

For this one-dimensional convolutional layer, 64 filters of 3×3 kernel-size were used.

A bi-LSTM layer with 128 hidden neurons is applied in the processing of sequential data, as it mitigates the exploding and vanishing gradient problem which recurrent neural network (RNN) fails to resolve. In addition to the input, output and forget gate [45], to include the future context bi-LSTM uses both the forward and backward propagation [46] which are stated below:

$$\overrightarrow{h}_t = f(W_{\overrightarrow{h}x} x_t + W_{\overrightarrow{h}\overrightarrow{h}} \overrightarrow{h}_{t-1} + b_{\overrightarrow{h}}) \tag{3}$$

$$\overleftarrow{h}_t = f(W_{\overrightarrow{h}x} x_t + W_{\overrightarrow{h}\overrightarrow{h}} \overleftarrow{h}_{t+1} + b_{\overrightarrow{h}}) \tag{4}$$

where x_t represents the t^{th} vector of input sequence, f is the activation function, h_t is the hidden sequence, W and b are the corresponding weight and bias respectively.

Apart from these layers, flatten layer is used for making the output of CNN compatible with the bi-LSTM. Dense layers with 100 hidden units were used for classification and activated using the softmax function. The softmax function used is defined as follows [47] where C is the number of classes of the model, and for a given class s_i, s_j is the summation of the score of all classes:

$$f(s)_i = \frac{e^{s_i}}{\sum_j^C e^{s_j}}. \tag{5}$$

The loss was calculated by applying categorical cross-entropy ($\mathcal{L}$) and Adam optimizer was employed for optimization of the

TABLE II
CLASS-WISE TEST STATISTICS

Test Statistics	HC	NON-MI	MI
True positive (TP)	1579	1353	7330
False positive (FP)	21	47	10
False negative (FN)	18	0	60
True negative (TN)	8722	8940	2940

TABLE III
PERFORMANCE COMPARISON OF THE PROPOSED METHOD AND WIDELY RECOGNIZED DL METHODS FOR THE SAME DATASET

Method	Class	Se (%)	Sp (%)	Precision (%)	Accu (%)	F1 Score (%)	OA/ Kappa/ F1 score
1D-CNN	HC	90.49	98.04	89.25	96.89	89.87	93.926%
	non-MI	88.78	96.96	80.29	95.96	84.32	0.864
	MI	95.52	93.67	97.55	95.01	96.52	90.24%
LSTM	HC	93.13	98.14	89.75	97.39	91.41	95.164%
	non-MI	95.73	96.97	78.78	96.84	86.43	0.890
	MI	95.44	97.86	99.21	96.07	97.29	91.71%
CNN-LSTM	HC	96.57	99.11	95.13	98.72	95.84	97.853%
	non-MI	99.53	98.61	91.00	98.72	95.07	0.952
	MI	97.84	99.37	99.75	98.26	98.79	97.85%
Proposed	HC	98.87	99.76	98.69	99.62	98.78	99.246%
	non-MI	100	99.48	96.64	99.55	98.29	0.983
	MI	99.19	99.66	99.86	99.32	99.52	98.86%

TABLE IV
OVERALL COMPARISON OF THE EXISTING STRATEGIES WITH THE PROPOSED METHOD

Process	#Lead[b]	#Class	Basis of evaluation	Results
Intra and inter-lead based attention model + Softmax [4]	12	5 (HC, non-MI, EMI, AMI, CMI)	patient-independent	Se = 97.60%, OA = 97.79%, F1 = 97.65%, kappa = 0.97
Multiple instance learning + SVM, KNN [5]	12	2 (MI, HC)	class based	Highest Se = 92.6% ± 0.65% (SVM), Highest Sp = 88.1% ±2.3% (KNN)
Empirical wavelet transform on basis of Fourier-Bessel series expansion + SVM [8]	12	2 (MI, HC)	class based	Accu = 99.97%, Se = 100%, Sp = 99.95%
Dignostic features such as multiscale wavelet energy and eigen values + SVM [9]	12	2 (MI, HC)	class based	Accu = 96.00%, Se = 93%, Sp = 99.00%
Naïve Bayes classifier [13]	12	2 (MI, HC)	class based	Accu = 94.74%
Harmonic phase distribution pattern + Logistic regression [16]	3	2 (MI, HC)	class based	Accu = 95.6%, Se = 96.5%, Sp = 92.7%
Multiple-feature-branch CNN + softmax [17]	12	2 (MI, HC)	class based	Accu = 99.95%, Sp = 99.90%, Se = 99.97%
Fuzzy information granulation, CNN + softmax [18]	4	2 (GAMI, HC)	patient-independent	Accu = 96.00%, Sp = 97.37%, Se = 95.40%
Deep CNN (without noise) + softmax [20]	1	2 (MI, HC)	class based	Accu = 95.22%, Sp = 94.19%, Se = 95.49%
MFB-CBRNN + softmax [25]	12	2 (MI, HC)	patient-independent	Accu = 93.08%, Sp = 86.29%, Se = 94.42%
Proposed method	12	3 (HC, non-MI, MI)	class based	OA = 99.246%, overall Se = 99.25%, overall Sp = 99.62%, kappa = 0.983, F1 = 98.86%

[b]#: number of

model. Multi-class categorical cross-entropy was calculated from [48] which states:

$$\mathcal{L} = -\frac{1}{N}\sum_{n=1}^{N}\sum_{k=1}^{K}(y_{n,k})\log(\hat{y}_{n,k}) \tag{6}$$

where $y_{n,k}$ and $\hat{y}_{n,k}$ are the true and predicted labels respectively. All the classes and samples are represented as K and N respectively. A batch size of 15 with 150 epochs was employed for training the proposed model. To achieve the minimum loss, learning rate of 0.00001 for each iteration, and for avoiding overfitting problem, L2 regularization of 0.001 was set.

III. RESULTS AND DISCUSSION

The proposed model in this paper can be said to have higher model interpretability than existing algorithms as this model not only detects non-MI class but also can advise the specialists of particular feature intervals and amplitudes.

A. Removal of Class Imbalance

In [25], binary classification (MI and HC) was accomplished by inserting the raw signal into their model which was also a combination of CNN and bi-LSTM. They achieved an overall accuracy of 93.08% with 13.71% of HC beats and only 5.58% of MI beats being misclassified. They pointed out the imbalanced apportioning of the database as the sole reason for this unintentional outcome although augmentation of HC was attained by oversampling. In our paper, as the chosen temporal features act as a general representation of any changes in the ECG, it can inherently learn even from the few amount of data of HC and non-MI. Besides in any automated DL model, the presence of a huge amount of raw data is a prerequisite as it learns the features and maps them to the output. Eventually, imbalance in any class can hamper this mapping of proper features. Thus the proposed DL model in this paper is guided to learn features readily so that it can map the output despite of an imbalanced dataset.

Class imbalance is dealt with over or under-sampling and the target matrix controls this sampling of data. A stratified sampling strategy introduces a more robust and general way of compensating the imbalance by maintaining similar class distribution in each subset instead of uniform probability distribution used in normal k-folds. This class distribution involves training and testing the model approximately on the same percentage of data from each class and so stratified k-fold in implemented in this paper. 5-fold cross-validation is repeated 20 times for greater stability of obtained performance.

B. Evaluation and Comparison With Other DL Strategies

Among the studies that included non-MI class, a state-of-art overall classification accuracy (OA), kappa, and macro-averaged F1 score of about 99.246%, 0.983, and 98.86%

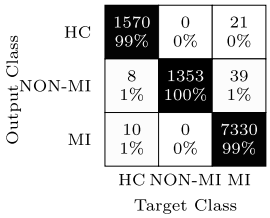

Fig. 7. Confusion matrix.

respectively were achieved using this proposed classification model. The detailed sample wise performance after application of 5-fold cross-validation is projected in Fig 7. Besides, the class-wise statistics as stated in table II are also very promising.

The performance of the model for each class was evaluated using parameters such as accuracy (Accu), sensitivity (Se), specificity (Sp), precision, and F1 score. The data obtained from table II is used for calculating the metrics exhibited in table III. The proposed model accomplished a superior outcome on all the assessment metrics and is verified using the similar dataset by comparing with diverse DL methods as enlisted in table III. As none of the subjects were falsely detected negative so we achieved a sensitivity of 100% in the non-MI class.

To the most of our knowledge, the only existing study that also classified non-MI subjects is [4]. They achieved an overall accuracy of 97.79%, kappa of 0.97, and F1 score of 97.65%. Besides, a brief comparison with all the other existing studies based on binary classification and localization of MI employing various strategies is listed in table IV. This table provides an outlook of the number of leads used, number of designated classes, and evaluation parameters of each study.

Considering all the facts stated above, it can be deduced that the proposed feature-based 12-lead CNN and the bi-LSTM model shows noteworthy improvement in performance for all of the classes. One of the fundamental reasons behind such success is the application of precise fiducial point detection methods. Moreover, as the algorithms are based on simple linear algebraic relations, it reduces the run time and complexity of implementation. Besides as the beat segmentation approach has been avoided, uncertainty of overlapping in training and test data set can be ensured and thus eluding optimistic results of classification.

IV. Conclusion

The unique architecture systematically processes 12-lead ECGs based on employing handcrafted features to discriminate the multiple classes present. The handcrafted features were selected on basis of their relativity of clinical perspective. The model merely does not diagnose diseases in addition to it, provides relevant information of features. Thus correlation of the feature values with the physical state of the patients provides a great hand for the specialists. Consequently, in the future on the need for new objective incorporation like introducing multiple classes of MI, the preferred features can be manipulated by feature selection methods. This method shows promising results if a selection of a minimum of 12 consecutive ECG cycles can be ensured for proper extraction of all the features used. However, with further research, the optimized number of consecutive ECG cycles required for this method can be determined to get an effective outcome. This model associated with a monitoring application can be converted in the future into a portable device which will help in early diagnosis and ensure appropriate treatment in due time.

References

[1] *The Atlas of Heart Disease and Stroke*, W. H. Organization, Geneva, Switzerland: 2004.
[2] W. H. Organization. (Jan. 14, 2021). *Cardiovascular Diseases (CVDs)*. [Online]. Available: https://www.who.int/en/news-room/fact-sheets/detail/cardiovascular-diseases-(cvds)
[3] *International Cardiovascular Disease Statistics*, S. F. Sheet-Populations, Amer. Heart Assoc., Dallas, TX, USA, 2004.
[4] E. Prabhakararao and S. Dandapat, "Myocardial infarction severity stages classification from ECG signals using attentional recurrent neural network," *IEEE Sensors J.*, vol. 20, no. 15, pp. 8711–8720, Aug. 2020.
[5] L. Sun, Y. Lu, K. Yang, and S. Li, "ECG analysis using multiple instance learning for myocardial infarction detection," *IEEE Trans. Biomed. Eng.*, vol. 59, no. 12, pp. 3348–3356, Dec. 2012.
[6] P. Kora and S. R. Kalva, "Improved bat algorithm for the detection of myocardial infarction," *SpringerPlus*, vol. 4, no. 1, p. 666, Dec. 2015.
[7] C. Han and L. Shi, "Automated interpretable detection of myocardial infarction fusing energy entropy and morphological features," *Comput. Methods Programs Biomed.*, vol. 175, pp. 9–23, Jul. 2019.
[8] R. K. Tripathy, A. Bhattacharyya, and R. B. Pachori, "A novel approach for detection of myocardial infarction from ECG signals of multiple electrodes," *IEEE Sensors J.*, vol. 19, no. 12, pp. 4509–4517, Jun. 2019.
[9] L. N. Sharma, R. K. Tripathy, and S. Dandapat, "Multiscale energy and eigenspace approach to detection and localization of myocardial infarction," *IEEE Trans. Biomed. Eng.*, vol. 62, no. 7, pp. 1827–1837, Jul. 2015.
[10] M. Arif, I. A. Malagore, and F. A. Afsar, "Detection and localization of myocardial infarction using K-nearest neighbor classifier," *J. Med. Syst.*, vol. 36, no. 1, pp. 279–289, Feb. 2012.
[11] A. Diker, Z. Cömert, and E. Avci, "A diagnostic model for identification of myocardial infarction from electrocardiography signals," *Bitlis Eren Univ. J. Sci. Technol.*, vol. 7, no. 2, pp. 132–139, Dec. 2017.
[12] U. R. Acharya *et al.*, "Automated detection and localization of myocardial infarction using electrocardiogram: A comparative study of different leads," *Knowl.-Based Syst.*, vol. 99, pp. 146–156, May 2016.
[13] N. Safdarian, N. J. Dabanloo, and G. Attarodi, "A new pattern recognition method for detection and localization of myocardial infarction using T-wave integral and total integral as extracted features from one cycle of ECG signal," *J. Biomed. Sci. Eng.*, vol. 7, no. 10, pp. 818–824, 2014.
[14] E. Alickovic and A. Subasi, "Medical decision support system for diagnosis of heart arrhythmia using DWT and random forests classifier," *J. Med. Syst.*, vol. 40, no. 4, p. 108, Apr. 2016.
[15] E. S. Jayachandran, K. P. Joseph, and U. R. Acharya, "Analysis of myocardial infarction using discrete wavelet transform," *J. Med. Syst.*, vol. 34, no. 6, pp. 985–992, Dec. 2010.
[16] D. Sadhukhan, S. Pal, and M. Mitra, "Automated identification of myocardial infarction using harmonic phase distribution pattern of ECG data," *IEEE Trans. Instrum. Meas.*, vol. 67, no. 10, pp. 2303–2313, Oct. 2018.
[17] W. Liu, Q. Huang, S. Chang, H. Wang, and J. He, "Multiple-feature-branch convolutional neural network for myocardial infarction diagnosis using electrocardiogram," *Biomed. Signal Process. Control*, vol. 45, pp. 22–32, Aug. 2018.
[18] W. Liu *et al.*, "Real-time multilead convolutional neural network for myocardial infarction detection," *IEEE J. Biomed. Health Informat.*, vol. 22, no. 5, pp. 1434–1444, Sep. 2018.
[19] R. K. Tripathy, A. Bhattacharyya, and R. B. Pachori, "Localization of myocardial infarction from multi-lead ECG signals using multiscale analysis and convolutional neural network," *IEEE Sensors J.*, vol. 19, no. 23, pp. 11437–11448, Dec. 2019.
[20] U. R. Acharya, H. Fujita, S. L. Oh, Y. Hagiwara, J. H. Tan, and M. Adam, "Application of deep convolutional neural network for automated detection of myocardial infarction using ECG signals," *Inf. Sci.*, vols. 415–416, pp. 190–198, Nov. 2017.
[21] N. Strodthoff and C. Strodthoff, "Detecting and interpreting myocardial infarction using fully convolutional neural networks," *Physiol. Meas.*, vol. 40, no. 1, Jan. 2019, Art. no. 015001.

[22] U. B. Baloglu, M. Talo, O. Yildirim, R. S. Tan, and U. R. Acharya, "Classification of myocardial infarction with multi-lead ECG signals and deep CNN," *Pattern Recognit. Lett.*, vol. 122, pp. 23–30, May 2019.
[23] O. S. Lih *et al.*, "Comprehensive electrocardiographic diagnosis based on deep learning," *Artif. Intell. Med.*, vol. 103, Mar. 2020, Art. no. 101789.
[24] K. Feng, X. Pi, H. Liu, and K. Sun, "Myocardial infarction classification based on convolutional neural network and recurrent neural network," *Appl. Sci.*, vol. 9, no. 9, p. 1879, May 2019.
[25] W. Liu, F. Wang, Q. Huang, S. Chang, H. Wang, and J. He, "MFB-CBRNN: A hybrid network for MI detection using 12-lead ECGs," *IEEE J. Biomed. Health Informat.*, vol. 24, no. 2, pp. 503–514, Feb. 2020.
[26] C. Han and L. Shi, "ML–ResNet: A novel network to detect and locate myocardial infarction using 12 leads ECG," *Comput. Methods Programs Biomed.*, vol. 185, Mar. 2020, Art. no. 105138.
[27] J. Zhang *et al.*, "Automated detection and localization of myocardial infarction with staked sparse autoencoder and treebagger," *IEEE Access*, vol. 7, pp. 70634–70642, 2019.
[28] X. Zhang, R. Li, H. Dai, Y. Liu, B. Zhou, and Z. Wang, "Localization of myocardial infarction with multi-lead bidirectional gated recurrent unit neural network," *IEEE Access*, vol. 7, pp. 161152–161166, 2019.
[29] S. M. Qaisar and A. Subasi, "Cloud-based ECG monitoring using event-driven ECG acquisition and machine learning techniques," *Phys. Eng. Sci. Med.*, vol. 43, no. 2, pp. 623–634, Jun. 2020.
[30] M. Hammad, A. M. Iliyasu, A. Subasi, E. S. L. Ho, and A. A. A. El-Latif, "A multitier deep learning model for arrhythmia detection," *IEEE Trans. Instrum. Meas.*, vol. 70, pp. 1–9, Oct. 2020, doi: 10.1109/TIM.2020.3033072.
[31] L. Hussain *et al.*, "Detecting congestive heart failure by extracting multimodal features and employing machine learning techniques," *BioMed. Res. Int.*, vol. 2020, pp. 1–19, Feb. 2020.
[32] P. D. Arini and E. R. Valverde, "Beat-to-beat electrocardiographic analysis of ventricular repolarization variability in patients after myocardial infarction," *J. Electrocardiol.*, vol. 49, no. 2, pp. 206–213, Mar. 2016.
[33] M. D'Aloia, A. Longo, and M. Rizzi, "Noisy ECG signal analysis for automatic peak detection," *Information*, vol. 10, no. 2, p. 35, Jan. 2019.
[34] J. Pan and W. J. Tompkins, "A real-time QRS detection algorithm," *IEEE Trans. Biomed. Eng.*, vol. BME-32, no. 3, pp. 230–236, Mar. 1985.
[35] N. Omar, M. Dey, and M. A. Ullah, "Detection of myocardial infarction from ECG signal through combining CNN and Bi-LSTM," presented at the in *Proc. 11th Int. Conf. Elect. Comput. Eng. (ICECE)*, Dec. 2020, pp. 395–398.
[36] R. Bousseljot, D. Kreiseler, and A. Schnabel, "Nutzung der EKG-signaldatenbank CARDIODAT der PTB über das Internet," *Biomedizinische Technik/Biomed. Eng.*, vol. 40, no. s1, pp. 317–318, Jul. 2009.
[37] A. L. Goldberger *et al.*, "PhysioBank, PhysioToolkit, and PhysioNet: Components of a new research resource for complex physiologic signals," *Circulation*, vol. 101, no. 23, pp. e215–e220, Jun. 2000.
[38] A. Abdullah, *ECG in Medical Practice*, 4th ed. Haryana, India: JP Medical Ltd, 2014.
[39] M. Cadogan. Jan. 1, 2021. *P Wave*. [Online]. Available: https://litfl.com/p-wave-ecg-library/
[40] L. G. Tereshchenko and M. E. Josephson, "Frequency content and characteristics of ventricular conduction," *J. Electrocardiol.*, vol. 48, no. 6, pp. 933–937, Nov. 2015.
[41] B. J. Kenny and K. N. Brown, *ECG T Wave*. Treasure Island, FL, USA: StatPearls, 2020.
[42] T. Pollehn, W. Brady, A. Perron, and F. Morris, "The electrocardiographic differential diagnosis of ST segment depression," *Emergency Med. J.*, vol. 19, no. 2, p. 129, 2002.
[43] P. W. Macfarlane, A. Van Oosterom, O. Pahlm, P. Kligfield, M. Janse, and J. Camm, *Comprehensive Electrocardiology*, 2nd ed. London, U.K.: Springer, 2010.
[44] H. B. Demuth, M. H. Beale, O. De Jess, and M. T. Hagan, *Neural Network Design*, 2nd ed. Stillwater, OK, USA: Martin Hagan, 2014.
[45] S. Hochreiter and J. Schmidhuber, "Long short-term memory," *Neural Comput.*, vol. 9, no. 8, pp. 1735–1780, 1997.
[46] M. Schuster and K. K. Paliwal, "Bidirectional recurrent neural networks," *IEEE Trans. Signal Process.*, vol. 45, no. 11, pp. 2673–2681, Nov. 1997.
[47] R. Gomez. (Jan. 2, 2021). *Understanding Categorical Cross-Entropy Loss, Binary Cross-Entropy Loss, Softmax Loss, Logistic Loss, Focal Loss and all Those Confusing Names*. [Online]. Available: https://gombru.github.io/2018/05/23/cross_entropy_loss/
[48] Y. LeCun, Y. Bengio, and G. Hinton, "Deep learning," *Nature*, vol. 521, pp. 436–444, May 2015.

Monisha Dey (Member, IEEE) is currently pursuing the B.Sc. degree in electrical and electronic engineering from the Chittagong University of Engineering and Technology (CUET), Chattogram, Bangladesh. She has keen interests in biomedical signal processing, deep learning, and robotics.

Nuzaer Omar (Member, IEEE) is currently pursuing the B.Sc. degree in electrical and electronic engineering with the Chittagong University of Engineering and Technology (CUET), Chattogram, Bangladesh. She has keen interests in signal processing, deep learning, and artificial intelligence.

Muhammad Ahsan Ullah (Member, IEEE) received the B.Sc. degree in electrical and electronic engineering (EEE) from the Chittagong University of Engineering and Technology (CUET), the M.Sc. degree from Kyung Hee University, South Korea, in 2007, and the Ph.D. degree from the Nagaoka University of Technology, Japan, in 2011. His research interests are digital signal processing, information and coding, wireless communications, control systems, image processing, the IoT, and embedded systems.